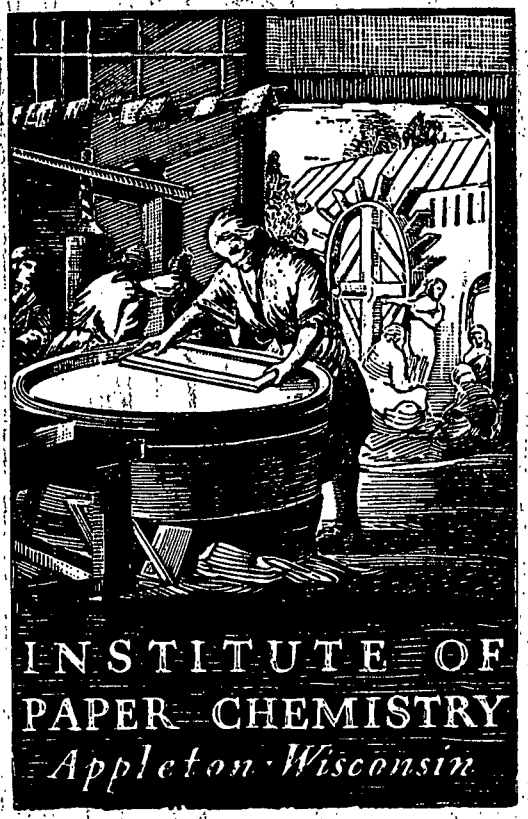

A FUNDAMENTAL RHEOLOGICAL STUDY OF THE BLADE COATING PROCESS

Project 3069

Report Two

A Progress Report

to

MEMBERS OF GROUP PROJECT 3069

August 9, 1974

THE INSTITUTE OF PAPER CHEMISTRY

Appleton, Wisconsin

A FUNDAMENTAL RHEOLOGICAL STUDY OF THE BLADE COATING PROCESS

Project 3069

Report Two

A Progress Report

to

MEMBERS OF GROUP PROJECT 3069

August 9, 1974

MEMBERS OF GROUP PROJECT 3069

Air Products & Chemicals Inc.

Appleton Papers Division, NCR Corporation

Blandin Paper Company

Champion International

Continental Can Co., Inc.

Eastex, Incorporated

Great Northern Paper Company

International Paper Company

The Mead Corporation

Scott Paper Company

Westvaco Corporation

Weyerhaeuser Company

TABLE OF CONTENTS

THE INSTITUTE OF PAPER CHEMISTRY

Appleton, Wisconsin

A FUNDAMENTAL RHEOLOGICAL STUDY OF THE BLADE COATING PROCESS

SUMMARY

Three lines of research have been followed: construction of a new rheometer; experimental coating evaluation; and the development of a new theory of nip flow.

Design of the new rheometer has been completed and construction is under way.

Alterations were made in the Blade Nip Rheometer to operate with 45° blades. Additional changes permitted the roll speed to be increased to 3000 ft/min and coating solids to be increased. Because of experimental difficulties and extensive downtime, a limited amount of experimental data was obtained. The quality of the data was generally poor and there is some question whether the wide angle blade will be useful in detailed coating evaluation. Some corrections to the machine have been made and the 45° blades will be tested again shortly. More stable operation is anticipated with the new rheometer and it may prove more useful in working with wide angle blades.

In prior work with 10° blades it was shown that the usual viscometric flow theory provides reasonable descriptions of the experimental results, except for highly viscoelastic coatings. In contrast, the results obtained with 45° blades show major divergence from the theory for all coatings tested. These results have emphasized the need for theory revision.

Relevant equations for a new theory have been developed and work is under way to solve them numerically with the computer. Terms contributing to nonviscometric flow in the momentum equations are included. A general constitutive equation is being used which is sufficiently simple to apply but is general enough to permit realistic description of common flows.

INTRODUCTION

The two basic goals of this research are: first, to develop means for measuring all pertinent rheological properties of coatings and to relate these properties to flow in coating nips; and second, to investigate the effect of coating formulation on rheological properties.

The object of this phase of the research was to pursue these goals on three fronts: to extend experimental parameters on the Blade Nip Rheometer to more realistically approximate actual coating conditions, to design and begin construction of a new rheometer which should extend the scope and quality of the rheological measurements, and to begin revision of current theory of nip flow in order to improve the description of flow in nips in terms of basic rheological parameters.

BACKGROUND

FLOW BEHAVIOR

The most commonly known flow is viscometric (often, if incorrectly, called simple shear). Viscometric flow can occur in various geometries but is usually illustrated as flow generated by laterally moving parallel plates (simple shear), as seen in Fig. 1. Viscometric flow is by definition steady state.

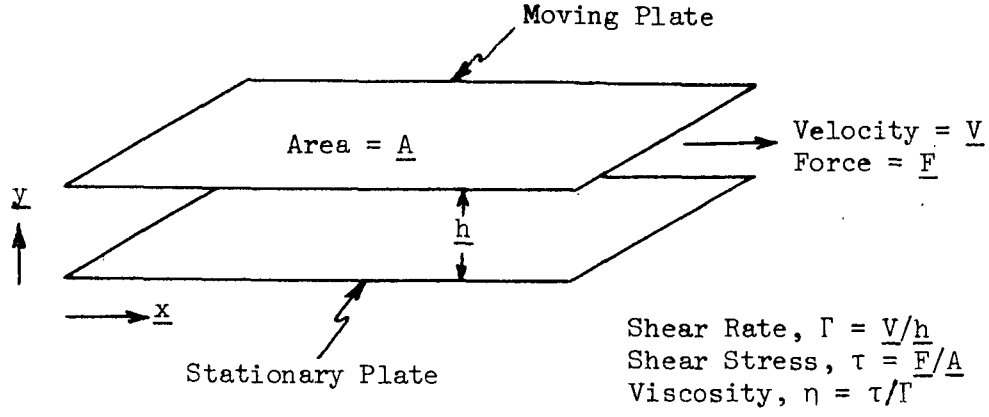

Figure 1. Simple Shear, a Viscometric Flow

There are of course important nonviscometric flows, for example turbulence and elongational flows. Examples of the latter are illustrated in Fig. 2.

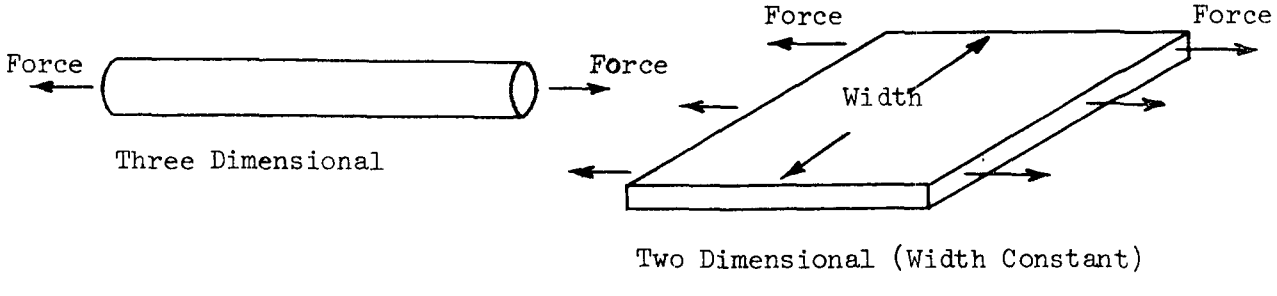

Figure 2. Illustrations of Elongational Flow

FLUID TYPES

One generally refers to three classes of fluid behavior: Newtonian: A fluid of constant viscosity in which the only stress occurring in viscometric flow is the shear stress, τ. Viscous: A fluid in which the viscosity may vary with shear rate, and in which the only stress component in viscometric flow is the shear stress. The Newtonian fluid is a special case of the viscous fluid. Viscoelastic fluid: A fluid in which normal stresses appear as well as the shear stress in viscometric flow. The result of the normal stresses in Fig. 1 would be to push the plates apart. Similarly, viscometric flow applied to blade nip flow predicts that viscoelastic normal stresses contribute to blade lift.

Some special terms frequently used include thixotropic, in which viscosity is reduced as a result of energy input into the fluid and viscosity recovers at rest; shear thinning, in which viscosity decreases with increasing shear rate in viscometric flow; and dilatant, in which viscosity increases with increasing shear rate in viscometric flow.

EXPERIMENTAL TERMS

The following symbols are used in subsequent discussions.

$\underline{V_o}$ = velocity of the Blade Nip Rheometer roll surface.

$\underline{h_o}$ = gap between the blade tip and the roll.

$\Gamma = \underline{V_o}/\underline{h_o}$ = approximate shear rate existing under the blade tip.

$\eta(\underline{D})$ = viscosity calculated from roll drag measurements.

$\eta(\underline{F})$ = viscosity calculated from normal blade load measurements.

For some purposes it is convenient to use experimental parameters without conversion to common units. Two of these, with conversion factors are as follows:

DX = drag exerted by the fluid on the roll.

F = normal force applied to the blades.

14.2 DX = force in grams.

480 F = force in grams.

EXPERIMENTAL PROCEDURES

It was desired in continued work to extend the experimental variables to more closely approximate those existing in commercial coaters by increasing coating solids, by using wider blade angles than the previous ten degree blades, and by increasing the roll velocity above the 2000 ft/min maximum used in prior work. These variable changes required alterations of the present Rheometer.

Blades with 45° angles were constructed and installed on the blade holder. The distance between blade tips and the vertical heights of the blades were unchanged from the previous ten degree blades [see Fig. 3 of Reference (1)]. The blades were ground in on the roll as was done earlier [(1) p. 21]. Unlike the 10° blades, it was necessary to hone the blades after grinding. The blade tips were ground to the following average values for the experiments:

Expt. 29: tip length = 0.148 cm

Expt. 30: tip length = 0.158 cm

Expt. 31: tip length = 0.160 cm.

The following procedures were used to prepare the coatings:

STARCH BINDER PREPARATION

Starch was slurried with deionized water at 39% solids. The starch was then cooked for 15 minutes by steam injection at a maximum temperature of 95°C. The cooked starch was then diluted to 25% solids.

PVA BINDER PREPARATION

The PVA was slowly added to water while stirring to make a 10% solids mix. The mixture was heated to 90°C with a closed steam coil until the PVA

dissolved, which was indicated by the solution becoming clear. The solution was cooled and adjusted to 10% solids by adding water.

CLAY SLIP PREPARATION

Experiments 29, 30, 31: The clay slip was blended for 30 minutes with a Lightnin' mixer at 71% solids, followed by 1 1/2 minutes in a large Waring Blendor.

Experiments 32, 33: A Hobart mixer was used for coating preparation in these experiments. Clay was added to water while mixing at low speed until 75% solids were attained. After mixing for 30 minutes at low speed, the slip was diluted to 71% solids and mixing was continued at medium speed for 20 minutes. Clay slips prepared by the two techniques were compared by Hercules viscosity and appearance in electron micrographs to confirm comparable results.

COATING PREPARATION

Binder solutions were slowly added to clay slips while stirring with a Lightnin' mixer (Experiments 29, 30, 31) or the Hobart mixer (Experiments 32, 33). The PVA binder was added especially slowly to avoid shock. After all binder was added, the coatings were mixed an additional 30 minutes.

Formulations and percentage solids of the coatings tested with 45° blades are given in Table I. Coatings used in qualitative scratching tests (Experiments 32, 33) are described later in Table II.

It was shown earlier how the springs which transmit normal force from the blade applicator to the blade holder are set off center to assure approximate equal normal force on the two blades [(1) p. 16-20]. The optimum spring locations

(neglecting the weight of blades and blade holder, which would have major effects only at the lower blade loads) are given by:

$$\Delta_3 - \Delta_2 = (DX/F)/4.82 \qquad (1)$$

in which Δ_3 is the distance of the bottom springs below center (cm) and Δ_2 is the distance of the top springs above center (cm). According to viscometric theory $\underline{DX}/\underline{F}$ for 45° blades should be about 20. For the first experiment (Expt. 29) $\Delta_3-\Delta_2$ was set at 4.0 cm, corresponding to $\underline{DX}/\underline{F}$ = 19.3. The experimental data gave values of $\underline{DX}/\underline{F}$ much lower due to inadequacy of the theory. The value 1.7 cm for $\Delta_3-\Delta_2$ was thus set for subsequent experiments, which corresponds to $\underline{DX}/\underline{F}$ of 8.2. It can be seen in the following results (Fig. 5 and 7) that this is a reasonable medial value.

TABLE I

COATINGS TESTED WITH 45° BLADES

Expt.	Coating	Formulation		Solids, %	Flow Rate[b]
29	29: low solids starch	KCS(S.D.) clay:	100 parts		
		Stayco M starch:	20 parts		
		Quadrafos:	0.1 part	53.0	130
30	301: low solids starch	KCS(S.D.) clay:	100 parts		
		Stayco M starch:	21 parts		
		Quadrafos:	0.1 part	53.0	120
30	302: high solids[a] starch	KCS(S.D.) clay:	100 parts		
		Stayco M starch:	21 parts		
		Quadrafos:	0.1 part	57.5	6
31	311: high solids starch	KCS(S.D.) clay:	100 parts		
		Stayco M starch:	21 parts		
		Quadrafos:	0.1 part	55.6	300[c]
31	312: high solids PVA	KCS(S.D.) clay:	100 parts		
		Du Pont Elvanol 71-30 PVA:	5 parts		
		Quadrafos:	0.1 part	54.4	300[c]

[a] No data taken due to low flow rate.
[b] Recirculation rate in ml/sec.
[c] Recirculation rate after new pump installed.

Anticipating larger values of DX/F than obtained with the ten degree blades, the voltmeter measuring DX from the SCR control drive was fitted with an optional switch to double the range. Even though drag readings were lower than anticipated, the option was used to extend the useful data range in testing high solids polyvinyl alcohol coating (Expt. 31).

No alteration was required to extend the roll surface velocity to 3000 ft/min.

Prior to Expt. 29, the coating circulation lines were enlarged and, where possible, shortened. Flow rates with low solids starch coatings (Expt. 29 and 30) gave delivery rates of 125-130 ml/sec to both blades, rates comparable to that obtained in prior work. The flow rate of high solids starch coating was too low to even consider data taking. In order to test higher solids coatings, the circulating pump was replaced by a Teel pump, Model 1P555, Dayton Electric Mfg. Co., Chicago. The pump is driven by a 1725 rpm, 1/2 hp motor, General Electric Model 5KC43MG635. It was found that the coating delivery rate for high solids starch and polyvinyl alcohol coatings was about 300 ml/sec. This is a satisfactory flow rate and the present system will presumably suffice for all subsequent work.

EXPERIMENTAL RESULTS

QUALITY OF THE EXPERIMENTAL DATA

It was previously determined that the major factor contributing to random scatter was the film thickness measurements, with measurements of roll drag, normal force, and roll velocity being minor contributors (1). Based on the limited data taken, the situation with 45° blades appears to be qualitatively similar.

In the first two experiments (29 and 30), the film thickness readings appeared to be subject to moderately greater random variations and vibrations than previously observed. The dial indicator was cleaned and oiled after Expt. 30 due to an apparent drift in static readings. In the last experiment (Expt. 31), the readings showed both large drift in base readings and very large amounts of vibration. The readings varied from not very accurate but useful to completely useless. A new dial indicator has been received and will be used in subsequent work.

VISCOUS HEATING CORRECTIONS

In prior work with 10° blades, corrections to experimental results were made for viscous heating effects [(1), Appendix IV]. The corrections were made assuming viscometric flow. The corrections were generally reasonable in magnitude. Calculations for 45° blades indicated moderate and reasonable corrections to $\eta(\underline{D})$ but very large corrections to $\eta(\underline{F})$. In fact, for some conditions of thin films at high speed, it was predicted that the normal force could be negative instead of positive. The reason for the differing effects on $\eta(\underline{D})$ and $\eta(\underline{F})$ is essentially that $\eta(\underline{D})$ is affected by reduced fluid viscosity

due to heating while $\eta(\underline{F})$ is affected by a change in velocity profile as well as the viscosity effect.

The experimental results for 45° blades showed large deviations from viscometric flow in a direction which would reduce the viscous heat effect. Because of the deviation from viscometric flow theory, the viscous heat program is considered unreliable for results obtained with 45° blades and the results were not corrected. As the theory is revised to better account for flow in wide blade angles, and viscous heating effects will also be revised, either as an integral part of the revised theory or, as was previously done, in separate calculations.

LOW SOLIDS STARCH COATING RESULTS

Calculated values of viscosity determined from roll drag $[\eta(\underline{D})]$ and blade lift $[\eta(\underline{F})]$ vs. shear rate under the blade tip, Γ, are presented in Fig. 3. The roll drag values are compared with previous results obtained with 10° blades in Fig. 4. The Hercules viscosity for the coatings of Experiments 29 and 30 was about 1.5 times as great as that obtained in earlier work. If the top three curves of Fig. 4 are lowered by this factor it appears that comparable viscosities are determined by roll drag with the two blade angles. As shear rate increases, the relative importance of flow under the blade tip increases compared with that under the blade surface. Since the assumption of viscometric flow is presumably more valid for flow under the blade tip than the blade surface, the greater divergence of the curves at lower shear rates is likely due to non-viscometric flow in the converging region.

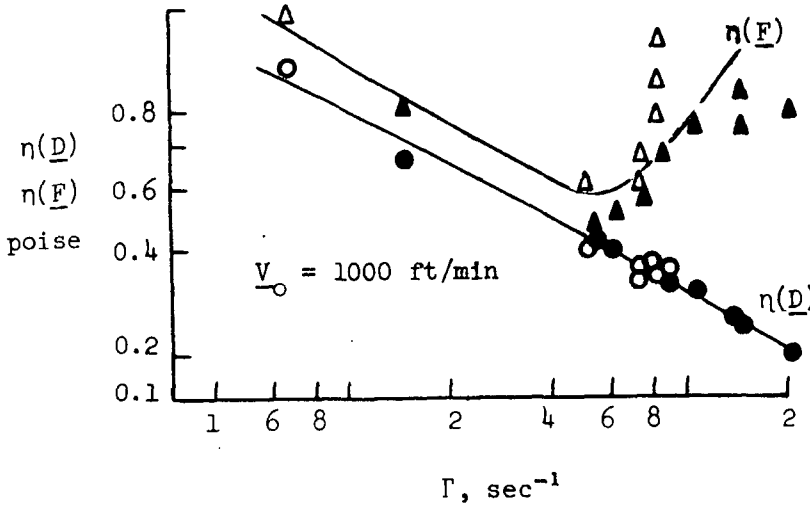

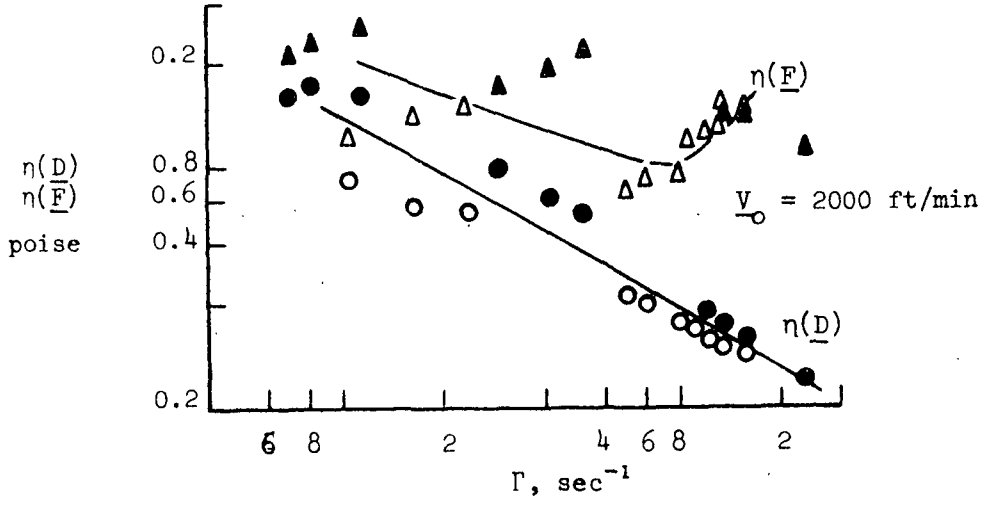

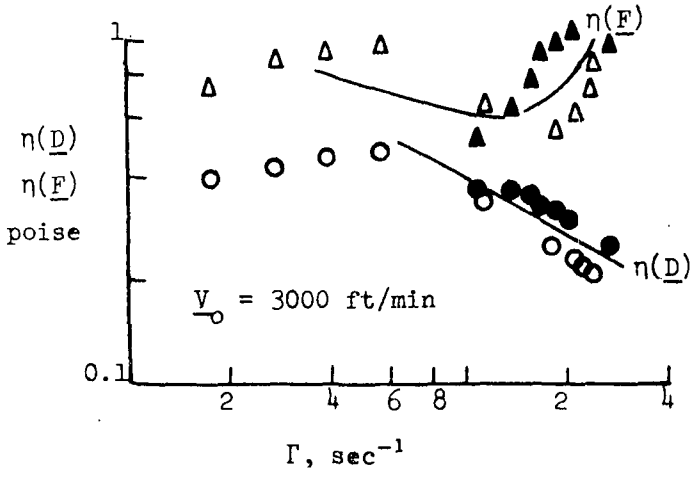

	η(F)	η(D)
Expt. 29	△	○
Expt. 30	▲	●

Power law exponent = 0.7
No viscous heat or cross-flow corrections
Blade angle = 45°

Figure 3. Rheometer Results for Low Solids Starch Coatings

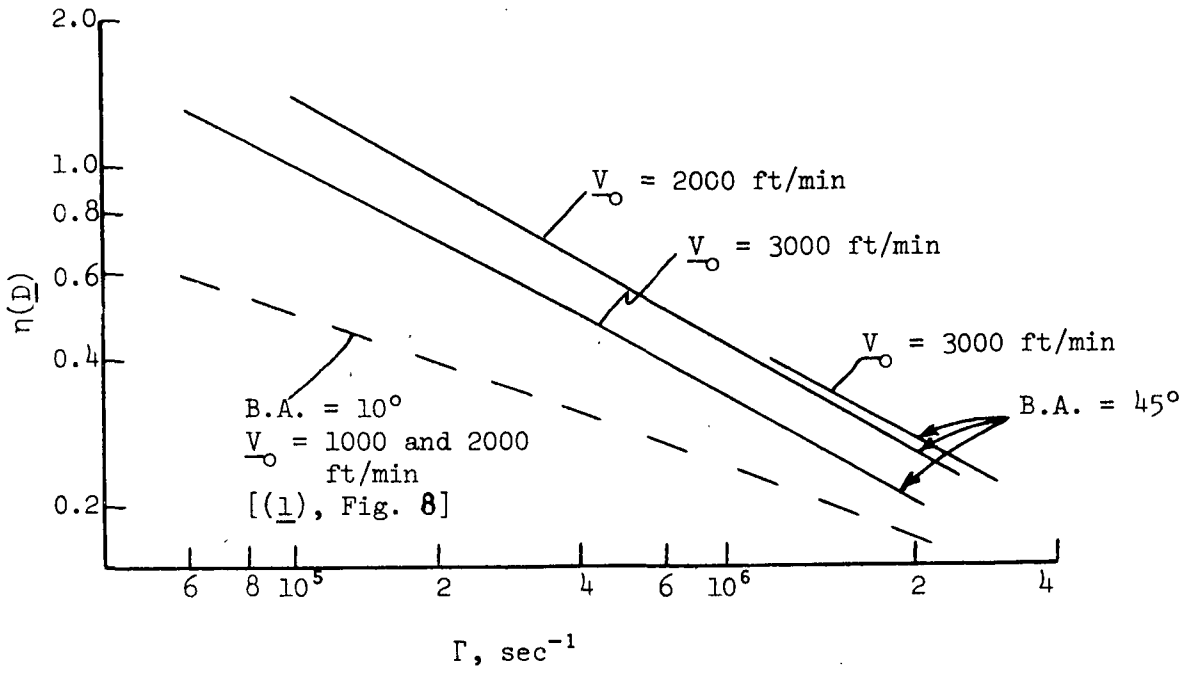

Figure 4. Comparison of $\eta(\underline{D})$ Results for 10° and 45° Blades for Low Solids Starch Coatings

The situation for blade lift viscosity, $\eta(\underline{F})$, is quite different. Here there is seen to be a radical divergence of results from what is predicted by viscometric flow theory. This is not as surprising as might at first seem. Even if flow under the blade tip is nearly viscometric, the pressure build up responsible for blade lift is a function of flow through the entire nip, even if the major contributor to lift is by the fluid under the tip. It can be shown mathematically that a small change in velocity profile under the blade tip can cause a major change in the pressure but a very minor change in the shear stress at the roll surface.

In practical terms, these results may be of considerable significance. They indicate that the free film coat weight in a blade coater may be several times as great as predicted by common viscometric flow theory, and indeed they may indicate that coat weight is quite insensitive to blade load for low coat

weights. It will be interesting to see how these results are affected by coating formulation and additives and by changes in blade angle.

The results of Fig. 3 are very much what one would expect for viscometric flow of a viscoelastic coating, with the excess blade lift being due to a normal stress contribution. This is considered unlikely due to the absence of similar results with 10° blades. Such results have spurred efforts to revise the theory, to provide better prediction of how a given coating will behave under specific conditions, and to enhance the value of blade nip measurements.

HIGH SOLIDS STARCH COATING RESULTS

Due to large vibrations and large drift in the dial indicator readings, the film thickness values for this coating are virtually meaningless. However, there is a method of presenting the remaining data from which some conclusions can be drawn. The ratio $\underline{DX}/\underline{F}$ is predicted by viscometric flow theory to be a very weak function of film thickness. This permits one to compare the high solids starch results with those obtained for low solids starch coatings. Consider the results plotted in Fig. 5. It seems reasonable to assume that the drag viscosity, $\eta(\underline{D})$, is an approximation to the true viscosity for the high solids starch coating. If so, divergence of the data in Fig. 5 from the theoretical lines would be due to divergence of blade lift viscosity, $\eta(\underline{F})$, from the theory. The high solids results display the same behavior as the low solids values, and it is concluded that the same general type of behavior may be expected for both coatings.

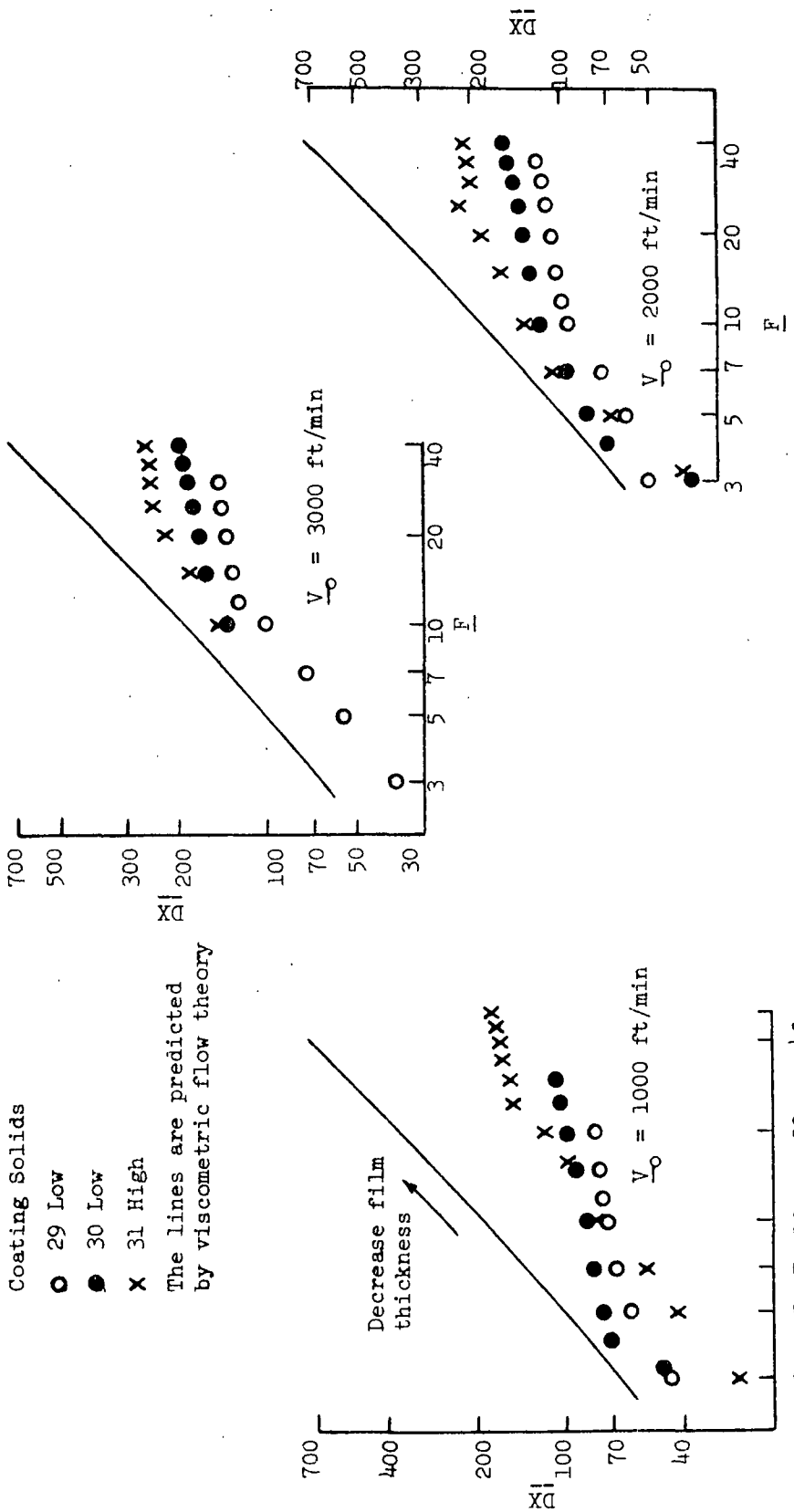

Figure 5. Comparison of Roll Drag vs. Blade Lift for Starch Coatings with Theory

POLYVINYL ALCOHOL COATING RESULTS

During Expt. 31 the dial indicator values vibrated badly resulting in poor precision of the readings. The static drift was reasonably low, however, so useful data were obtained except at 3000 ft/min.

The resulting viscosity values are presented in Fig. 6. In these results both $\eta(\underline{D})$ and $\eta(\underline{F})$ show much higher values than expected from viscometric flow theory, a result comparable to earlier results on PVA using 10° blades [(1), Fig. 20A and 20B]. This behavior was earlier attributed to nonviscometric flow, not just to normal stress blade lift, and the same is presumably true of the results obtained with 45° blades. There is, however, one difference between results obtained with 10 and 45° blades. It can be seen from earlier results that $\eta(\underline{D})$ is generally larger than $\eta(\underline{F})$ for 10° blades [(1), Fig. 20A and 20B]. A plot of $\underline{DX}$ vs. $\underline{F}$ for the current data is compared with viscometric flow theory in Fig. 7. It is clear from this figure that for the 45° blades $\eta(\underline{F})$ is slightly larger than $\eta(\underline{D})$. These results presumably illustrate the nonviscometric contributions of both viscous fluid properties (as seen with the starch coatings) and that due to viscoelastic properties (as seen with earlier results with PVA). Of course, the two factors cannot be so easily separated, except in a qualitative sense.

A BLADE SCRATCHING OBSERVATION

The Rheometer roll develops pits and cracks after extended use. These defects provide holes in which pigment particles catch and cause local scratching of blades. The process accelerates and eventually requires replating of the roll.

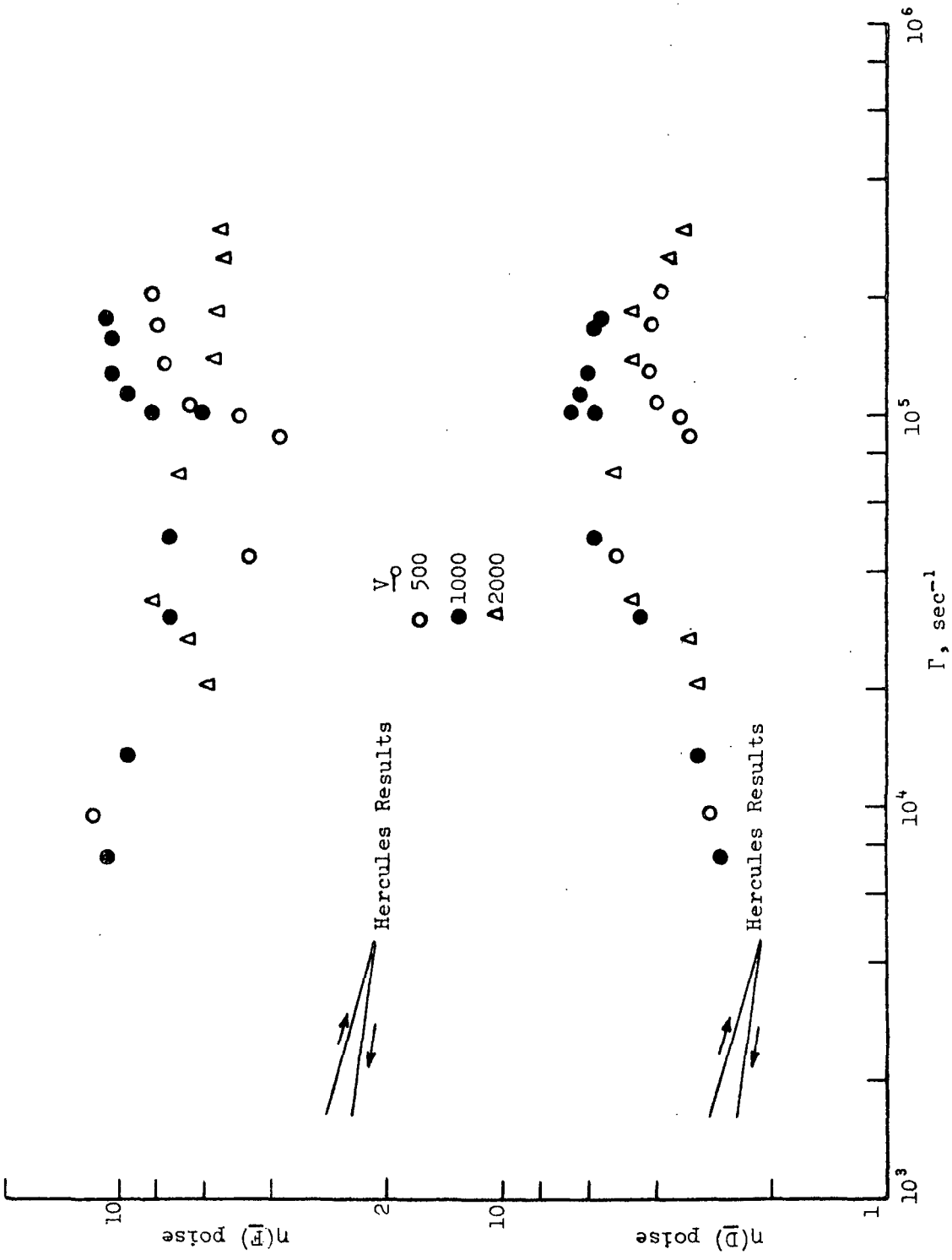

Figure 6. Polyvinyl Alcohol Coating Results (Expt. 31)

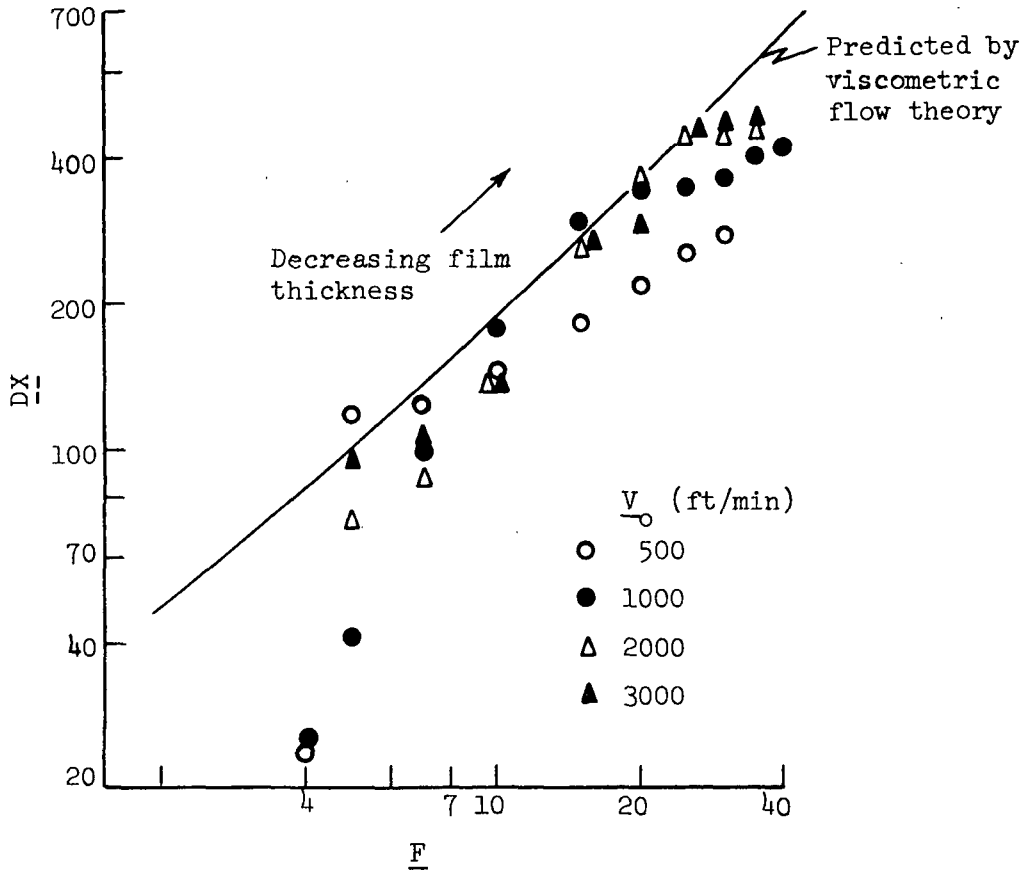

Figure 7. Plot of Blade Lift (F) vs. Roll Drag (DX) for Polyvinyl Alcohol Coating

A quite different type of scratching was observed after Expt. 31 in which high solids starch and high solids polyvinyl alcohol coatings were tested. Both roll and blades were severely scratched across the entire width. The roll had been replated just before this experiment and it appeared that a unique scratching phenomena had occurred. It was considered possible that the high solids polyvinyl alcohol coating, which is known to cause blade scratching in commercial coating, was responsible. It might be that the nature of the polyvinyl alcohol binder is such that under appropriate conditions of formulation and fluid deformation the pigment suspension is broken and particles are released which cause scratching.

Two experiments were conducted to attempt a repeat of the scratching phenomena. The blades were ground in on the roll using Carborundum powder slurry until most of the scratches were considerably reduced in severity. The testing conditions are given in Table II. The dramatic scratching observed after Expt. 31 was not reproduced however. This phenomenon is considered of sufficient importance to warrant further study under more closely controlled conditions. Due to the time and expense of replating of the roll, this will be done with the new rheometer being constructed.

CONSTRUCTION OF A NEW RHEOMETER

In accordance with the project proposal (2) a new rheometer has been designed and construction is under way.

The following description of the major operating principles of the machine makes reference to the front view shown in Fig. 8. The fluid is contained in the temperature-controlled cavity 1 which is part of the bottom plate assembly. The fluid is sheared between the circular top plate 2 and blades or a ring attached to the bottom plate 3. The top plate rotates but has no vertical movement. The bottom plate is free to move vertically but is prohibited from rotating. In order to permit near perfect fit of the shearing surfaces, the bottom plate is also permitted to "float" by means of the gimbal bearing 4. Normal force is applied to the bottom plate with a hydraulic ram 5. The force is transmitted by a beam 6 and is measured by a sensing device 7. The torque applied to the bottom plate is measured by a beam 8 and a sensing device 9. The film thickness is measured by means of a sensing device 10 which is a permanent part of the lower plate assembly. The top plate rotational speed is measured by sensing device 11.

TABLE II

CONDITIONS USED IN BLADE-ROLL SCRATCHING TESTS

Binder[a]	Solids, %	Roll Velocity, ft/min	F	Time of Test, min
		Experiment 32		
Starch	50.1	2000	25	5
Starch	56.1	2000	50	5
PVA	50.9	2000	50	5
PVA	52.9	2000	50	5
		1000	40	5
		500	30	5
		1000	40	1/4
		500	40	1/4
		250	40	1/4
		125	40	1/4
		Experiment 33		
PVA	54.6	2000	50	5
		500	50	5
		1000	50	5
PVA-starch[b]	54.4	1000	50	5
		500	50	5

[a] Binder and pigment properties are given in Table I. The binder-pigment ratios are the same as given for Expt. 31.

[b] 20% of the PVA coating was replaced with high solids starch coating to determine if the combined binders had an effect.

A schematic of the electronic equipment required for the measurements is shown in Fig. 9.

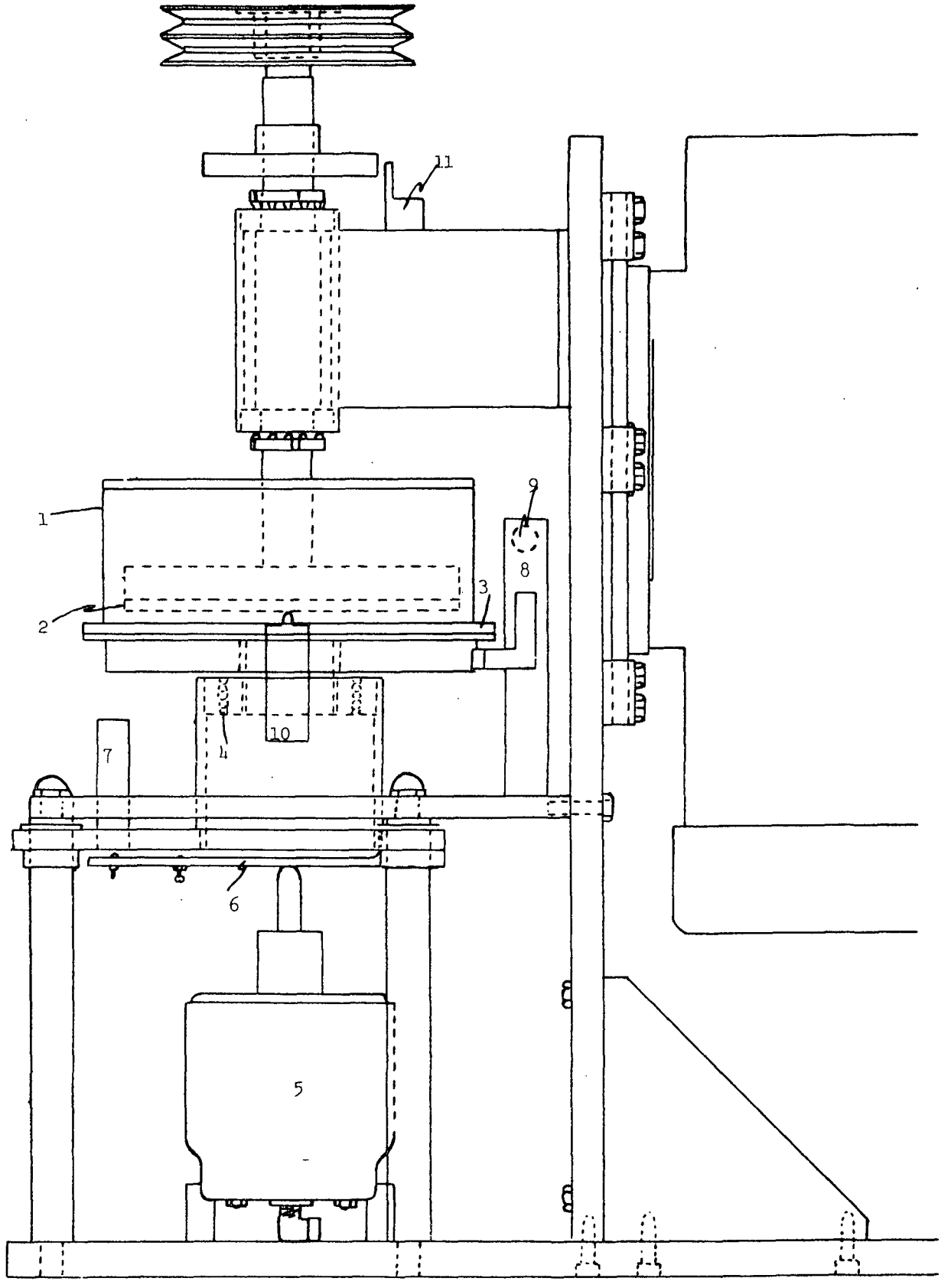

Figure 8. Front View of the New Rheometer

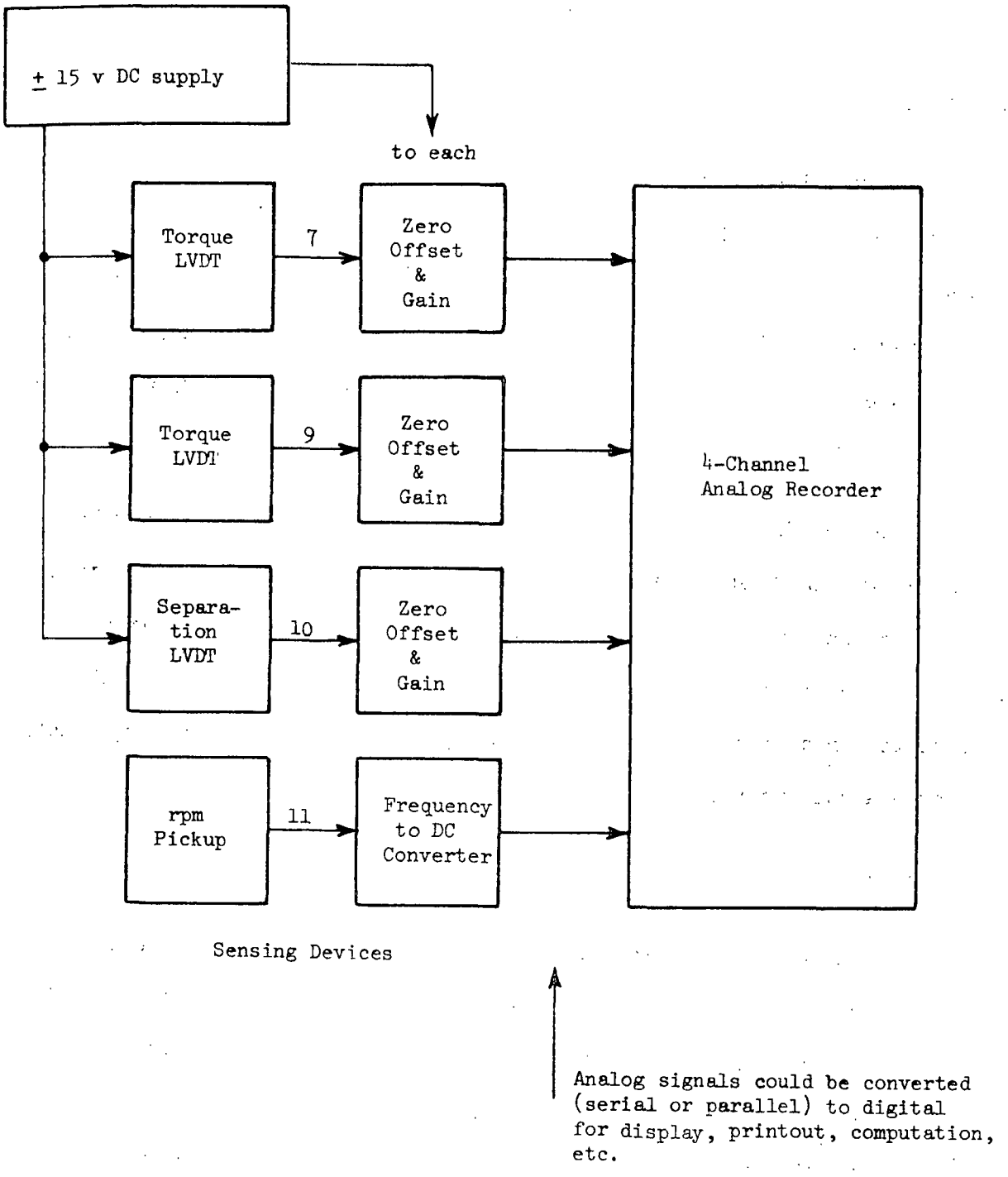

Figure 9. Sensing Devices and Auxiliary Electronic Equipment

THEORY REVISION

INTRODUCTION

It was shown in previous work with ten degree blades that, except for highly viscoelastic coatings, there was reasonable conformity of the results to viscometric flow theory. The current results obtained with 45° blades suggests that one cannot expect satisfactory conformity to the theory for any coating in wide blade angle flow. The development of a valid theory for blade nip flow has thus become of considerable importance.

The new theory involves nonviscometric flows and a nonrectangular coordinate system. These complexities require that the mathematical analysis be in tensor form and it is possible that the details will be of limited interest to some readers. Those interested might refer to Spiegel for the basics of tensor analysis (3) and to Flügge (4) and Aris (5) for the application of tensor analysis to rheology.

COORDINATE SYSTEMS

One is concerned here with two-dimensional flow. While cross flow out the ends of the nip does occur, it is neglected in the analysis. The normal stress in the cross direction is finite and is not neglected but, since all derivatives in the cross direction are assumed zero, nothing is lost in dealing with a two-dimensional coordinate system. Only when the stress tensor is considered will the system be three dimensions and, in that case, the third dimension is considered rectangular and adds no complications. The x, or 1, coordinate direction will be considered to be in the general direction along the nip and the y, or 2, coordinate will be across the film.

One is concerned here with two types of coordinates: Cartesian (rectangular), in which the coordinate lines are straight lines mutually perpendicular, and a general orthogonal, in which the coordinate lines are of arbitrary curvature and mutually perpendicular. These coordinates are illustrated in Fig. 10.

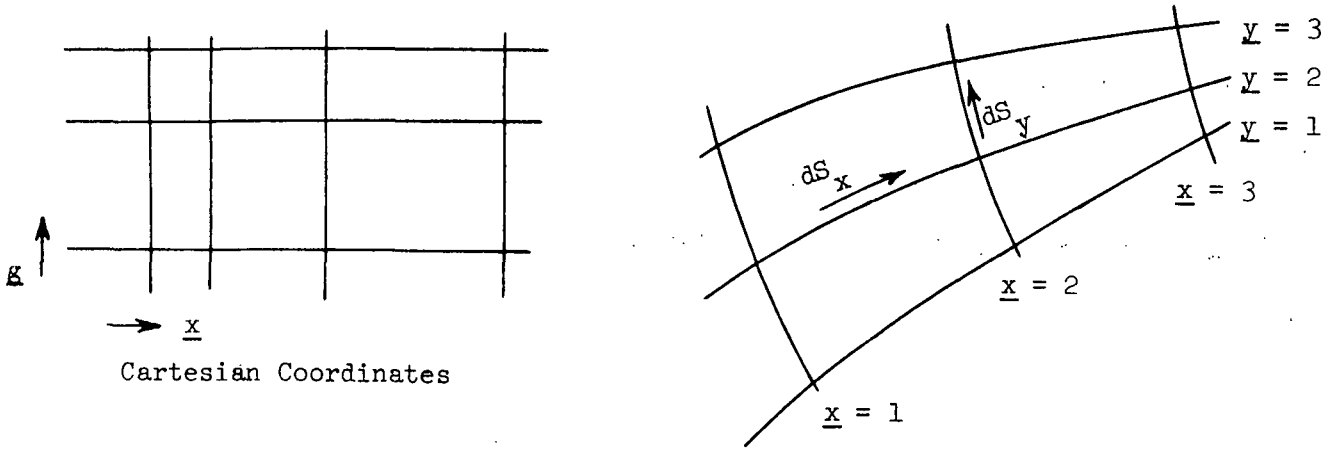

Figure 10. Coordinate Systems

A coordinate system is completely defined by the metric tensor, g_{ij}, which is a function of position. The metric tensor is defined as follows:

$$ds^2 = g_{ij}\, dx^i\, dx^j \tag{2}$$

Since the components g_{ij} are zero for orthogonal coordinates when $i \neq j$,

$$g_{ii} = (ds/dx^i)^2 \tag{3}$$

in which ds/dx^i is the differential physical arc length per differential coordinate change for the i coordinate. In the general orthogonal coordinates to be considered, the coordinates are dimensionless and g_{ii} has the dimensions of length^2.

In the usual Cartesian coordinates the distance between coordinate lines is unity and the diagonal metric tensor components are dimensionless and equal to one. For unequal distances between lines, as shown in Fig. 10, it is a trivial decision whether one uses a metric tensor or defines derivatives and integrals in terms of the physical coordinates. The latter procedure was followe in prior work [(1), Appendix I-IV].

KINEMATIC TENSORS

Two kinematic tensors are of interest: the deformation rate tensor, $\underline{\underline{E}}^{ij}$, and the vorticity tensor, $\underline{\underline{W}}^{ij}$, defined as follows:

$$E^{ij} = 1/2\ (g^{jk}\ v^{i}_{\ ,k} + g^{ik}\ v^{j}_{\ ,k}) \tag{4}$$

$$W^{ij} = 1/2\ (g^{ik}\ v^{j}_{\ ,k} - g^{jk}\ v^{i}_{\ ,k}) \tag{5}$$

in which $\underline{v}^{i}_{\ ,\underline{k}}$ indicate the covariant derivative, and there is the usual summatio of indices. In matrix notation:

$$\underline{\underline{E}} = \begin{pmatrix} e_1 & e & o \\ e & -e_1 & o \\ o & o & o \end{pmatrix} \tag{6}$$

$$\underline{\underline{W}} = \begin{pmatrix} o & w & o \\ -w & o & o \\ o & o & o \end{pmatrix} \tag{7}$$

The components of Equations (6) and (7) are as follows:

	General Orthogonal Coord.	Cartesian Coord.	Viscometric Flow Cartesian Coord.	
e	$= 1/2\left(\frac{1}{\Delta}\frac{\partial u}{\partial x} + \frac{1}{\delta}\frac{\partial v}{\partial y} - \frac{u}{\Delta\delta}\frac{\partial \delta}{\partial x} - \frac{v}{\Delta\delta}\frac{\partial \Delta}{\partial y}\right)$	$1/2\left(\frac{\partial u}{\partial x} + \frac{\partial v}{\partial y}\right)$	$1/2\frac{\partial v}{\partial y} = 1/2\,\Gamma$	(8)
e_1	$= \frac{1}{\Delta}\frac{\partial v}{\partial x} + \frac{u}{\Delta\delta}\frac{\partial \Delta}{\partial y} = -\frac{1}{\delta}\frac{\partial u}{\partial y} - \frac{v}{\Delta\delta}\frac{\partial \delta}{\partial x}$	$\frac{\partial v}{\partial x} = -\frac{\partial u}{\partial y}$	0	(9)
w	$= 1/2\left(\frac{1}{\Delta}\frac{\partial u}{\partial x} - \frac{1}{\delta}\frac{\partial v}{\partial y} + \frac{u}{\Delta\delta}\frac{\partial \delta}{\partial x} - \frac{v}{\Delta\delta}\frac{\partial \Delta}{\partial y}\right)$	$1/2\left(\frac{\partial u}{\partial x} - \frac{\partial v}{\partial y}\right)$	$-1/2\frac{\partial v}{\partial y} = -1/2\,\Gamma$	(10)

in which $\Delta = \sqrt{g_{11}}$

$\delta = \sqrt{g_{22}}$

$\underline{v} = \underline{v}^1$

$\underline{u} = \underline{v}^2$

$\underline{x} = \underline{x}^1$

$\underline{y} = \underline{x}^2$

Γ = shear rate in viscometric flow.

At this point the subscripts and superscripts $\underline{1}$ and $\underline{2}$ can be arbitrary. It will be seen later (Fig. 11) that $\underline{1}$ is chosen as the direction along the nip and $\underline{2}$ is across the film.

STRESS TENSORS

Two stress tensors are defined as follows:

$$\underline{\underline{S}} = \text{deviatoric stress tensor} = \begin{pmatrix} P_{11} & \tau & o \\ \tau & P_{22} & o \\ o & o & P_{33} \end{pmatrix} \qquad (11)$$

$$\underline{\underline{\tau}} = \text{total stress tensor} = \begin{pmatrix} \tau_{11} & \tau & o \\ \tau & \tau_{22} & o \\ o & o & \tau_{33} \end{pmatrix} = \underline{\underline{S}} - p \begin{pmatrix} 1 & o & o \\ o & 1 & o \\ 0 & 0 & 1 \end{pmatrix} \quad (12$$

in which $\underline{p}$ is the hydrostatic pressure.

The normal stresses $\underline{P}_{11}$, $\underline{P}_{22}$, and $\underline{P}_{33}$ are unique functions of the fluid kinematics. The pressure, $\underline{p}$, and thus the normal stresses τ_{11}, τ_{22}, and τ_{33} are not unique functions of the kinematics but depend on external boundary conditions. The total normal stresses are physical values imposed on an element of fluid from an external boundary. Both types of normal stresses have the sense of tension. For all fluids in all types of flow:

$$P_{11} + P_{22} + P_{33} = 0 \quad (13$$

It is convenient to define two normal stress differences:

$$P = P_{11} - P_{22} \quad (14$$

$$Z = P_{22} - P_{33} \quad (15$$

For the special case of viscometric flow, $\underline{P}_{11}$-$\underline{P}_{22}$ is called the first normal stress difference and is always positive for a viscoelastic fluid and zero for a viscous fluid, $\underline{P}_{22}$-$\underline{P}_{33}$ is called the second normal stress difference and can be positive or negative and is generally considered to be much less than the first normal stress difference, and τ is the shear stress.

THE EQUATION OF CONTINUITY

Assuming constant fluid density the equation of continuity in tensor notation is:

$$v^{i}{}_{,i} = 0 \quad (16$$

which results in:

General Orthogonal Coord.	Cartesian Coord.	Viscometric Flow Cartesian Coord.	
$\frac{1}{\Delta}\frac{\partial v}{\partial x} + \frac{1}{\delta}\frac{\partial u}{\partial y} + \frac{u}{\Delta\delta}\frac{\partial \Delta}{\partial y} + \frac{v}{\Delta\delta}\frac{\partial \delta}{\partial x} = 0$	$\frac{\partial v}{\partial x} + \frac{\partial u}{\partial y} = 0$	$\frac{\partial v}{\partial x} = 0 \quad u = 0$	(17)

THE MOMENTUM EQUATIONS (STEADY STATE, NO BODY FORCE)

In tensor notation the momentum equation is:

$$S^{ij}{}_{,j} - g^{ij}\, p_{,j} = \rho\, v^j\, v^i{}_{,j} \tag{18}$$

which results in the following:

For General Orthogonal Coordinates:

$$\frac{1}{\Delta}\frac{\partial \tau_{11}}{\partial x} + \frac{1}{\delta}\frac{\partial \tau}{\partial y} + 2\,\frac{\tau}{\Delta\delta}\frac{\partial \Delta}{\partial y} + \frac{P}{\Delta\delta}\frac{\partial \delta}{\partial x} = \rho\left[\frac{v}{\Delta}\frac{\partial v}{\partial x} + \frac{u}{\delta}\frac{\partial v}{\partial y} + \frac{uv}{\Delta\delta}\frac{\partial \Delta}{\partial y} - \frac{u^2}{\Delta\delta}\frac{\partial \delta}{\partial x}\right] \tag{19}$$

$$\frac{1}{\delta}\frac{\partial \tau_{11}}{\partial y} - \frac{1}{\delta}\frac{\partial P}{\partial y} + \frac{1}{\Delta}\frac{\partial \tau}{\partial x} + 2\,\frac{\tau}{\Delta\delta}\frac{\partial \delta}{\partial x} - \frac{P}{\Delta\delta}\frac{\partial \Delta}{\partial y} = \rho\left[\frac{v}{\Delta}\frac{\partial u}{\partial x} + \frac{u}{\delta}\frac{\partial u}{\partial y} + \frac{uv}{\Delta\delta}\frac{\partial \delta}{\partial x} - \frac{v^2}{\Delta\delta}\frac{\partial \Delta}{\partial y}\right] \tag{20}$$

For Cartesian Coordinates:

$$\frac{\partial \tau_{11}}{\partial x} + \frac{\partial \tau}{\partial y} = \rho\left(v\frac{\partial v}{\partial x} + u\frac{\partial v}{\partial y}\right) \tag{21}$$

$$\frac{\partial \tau_{11}}{\partial y} - \frac{\partial P}{\partial y} + \frac{\partial \tau}{\partial x} = \rho\left(v\frac{\partial u}{\partial x} + u\frac{\partial u}{\partial y}\right) \tag{22}$$

For Viscometric Flow in Cartesian Coordinates:

$$\frac{\partial \tau}{\partial y} = \frac{dp}{dx} \tag{23}$$

$$\frac{\partial(\tau_{11} - P)}{\partial y} = 0 = \frac{\partial \tau_{22}}{\partial y} \tag{24}$$

in which ρ is the fluid density.

THE CONSTITUTIVE EQUATION

A useful constitutive equation must have at least three characteristic

1) It must be a properly formulated tensor equation.
2) It must be sufficiently simple to permit application to the problem being considered.
3) It must predict reasonable results for simple flows, particularly for viscometric flow.

The equation to be used is an empirical Maxwell type equation with two (or three) variable coefficients. The derivation of the equation can be seen (6). The equation completely describes viscometric flow results and it is sufficiently simple to be applied to the present problem. In tensor notatio the equation is:

$$S^{ij} + \lambda \frac{\delta S^{ij}}{\delta t} - \beta\lambda \left(g_{kr} E^{ir} S^{kj} + g_{kr} S^{ir} E^{kj}\right) + \frac{2}{3} \lambda\beta\delta^{ij} g_{kr} g_{al} E^{ar} S^{kl} = 2\bar{\eta} E^{ij}$$

in which: (

$$\frac{\delta S^{ij}}{\delta t} = v^k S^{ij}{}_{,k} + g_{kr} W^{ir} S^{kj} + g_{kr} W^{jr} S^{ki}$$

The coefficients λ and $\bar{\eta}$ are considered to be functions of the second invariant of the deformation rate tensor, $II_{\underline{E}}$. The coefficient β can be a variable as we but generally will be considered constant. The second invariant is defined by:

$$II_E = -g_{ir} g_{jk} E^{jr} E^{ik}/2 \quad ($$

Three independent equations result from Equation (25). These equatic plus the invariant are:

For General Orthogonal Coordinates:

11-22

$$P + \lambda\left(\frac{v}{\Delta}\frac{\partial P}{\partial x} + \frac{u}{\delta}\frac{\partial P}{\partial y}\right) + \frac{4\lambda\tau}{\Delta\delta}\left(v\frac{\partial \Delta}{\partial y} - u\frac{\partial \delta}{\partial x}\right) + 4\lambda w\tau - \frac{2}{3}\beta\lambda e_1 (P+2Z) = 4\bar{\eta}e_1 \quad (27)$$

22-33

$$Z + \lambda\left(\frac{v}{\Delta}\frac{\partial Z}{\partial x} + \frac{u}{\delta}\frac{\partial Z}{\partial y}\right) + \frac{2\lambda\tau}{\Delta\delta}\left(u\frac{\partial \delta}{\partial x} - v\frac{\partial \Delta}{\partial y}\right) - 2\lambda w\tau - \frac{2}{3}\beta\lambda e_1 (P-Z) - 2\beta\lambda e\tau = -2\bar{\eta}e_1, \quad (28)$$

12

$$\tau + \lambda\left(\frac{v}{\Delta}\frac{\partial \tau}{\partial x} + \frac{u}{\delta}\frac{\partial \tau}{\partial y}\right) + \frac{\partial P}{\Delta\delta}\left(u\frac{\partial \delta}{\partial x} - v\frac{\partial \Delta}{\partial y}\right) - \lambda w P - \frac{1}{3}\beta\lambda e (P + 2Z) = 2\bar{\eta}e. \quad (29)$$

$$II_E = -(e^2 + e_1{}^2) \quad (30)$$

For Cartesian Coordinates:

$$P + \lambda\left(v\frac{\partial P}{\partial x} + u\frac{\partial P}{\partial y}\right) + 4\lambda w\tau - \frac{2}{3}\beta\lambda e_1 (P + 2Z) = 4\bar{\eta}e_1 \quad (31)$$

$$Z + \lambda\left(v\frac{\partial Z}{\partial x} + u\frac{\partial Z}{\partial y}\right) - 2\lambda w\tau - \frac{2}{3}\beta\lambda e_1 (P - Z) - 2\beta\lambda e\tau = -2\bar{\eta}e_1 \quad (32)$$

$$\tau + \lambda\left(v\frac{\partial \tau}{\partial x} + u\frac{\partial \tau}{\partial y}\right) - \lambda w P - \frac{1}{3}\beta\lambda e (P + 2Z) = 2\bar{\eta}e \quad (33)$$

$$II_E = -(e^2 + e_1{}^2) \quad (34)$$

For Viscometric Flow in Cartesian Coordinates:

$$P = 2\lambda\Gamma\tau \quad (35)$$

$$Z = -\lambda\Gamma\tau + \beta\lambda\Gamma\tau \quad (36)$$

$$\tau + \frac{1}{2}\lambda\Gamma P - \frac{1}{6}\beta\lambda\Gamma (P + 2Z) = \bar{\eta}\Gamma \quad (37)$$

$$II_E = -\frac{1}{4}\Gamma^2 \quad (38)$$

Solving for the Coefficients:

$$\beta = 1 + \frac{2Z}{P} \tag{39}$$

$$\lambda = \frac{P}{2\Gamma\tau} \tag{40}$$

$$\bar{\eta} = \frac{\tau}{\Gamma} + \frac{P^2}{6\Gamma\tau} \tag{41}$$

For a Viscous Fluid in General Orthogonal Coordinates:

$$P = 4\bar{\eta}e_1 \tag{42}$$

$$Z = -2\bar{\eta}e_1 \tag{43}$$

$$\tau = 2\bar{\eta}e \tag{44}$$

TECHNIQUE FOR SOLVING THE PROBLEM

An orthogonal coordinate grid is imposed on the nip as indicated in Fig. 11.

The boundary conditions are as follows:

$$\text{at } y = 1\text{: } v = -V_o \quad u = 0 \qquad \text{at } y = KK\text{: } v = u = 0 \tag{45}$$

$$\text{at } x = 1\text{: } \tau_{11} = 0 \text{ on the line K which has the minimum value of } -II_E$$
$$\text{at } x = JJ\text{: } \tau_{11} = 0 \text{ on the line K which has the minimum value of } -II_E \tag{46}$$

For justification of boundary condition (46) see Ref. (1), p. 120-121.

The initial attempt at solution is being done for a viscous fluid. The technique is such that a minimum of alteration will be required to extend to the more general viscoelastic fluid.

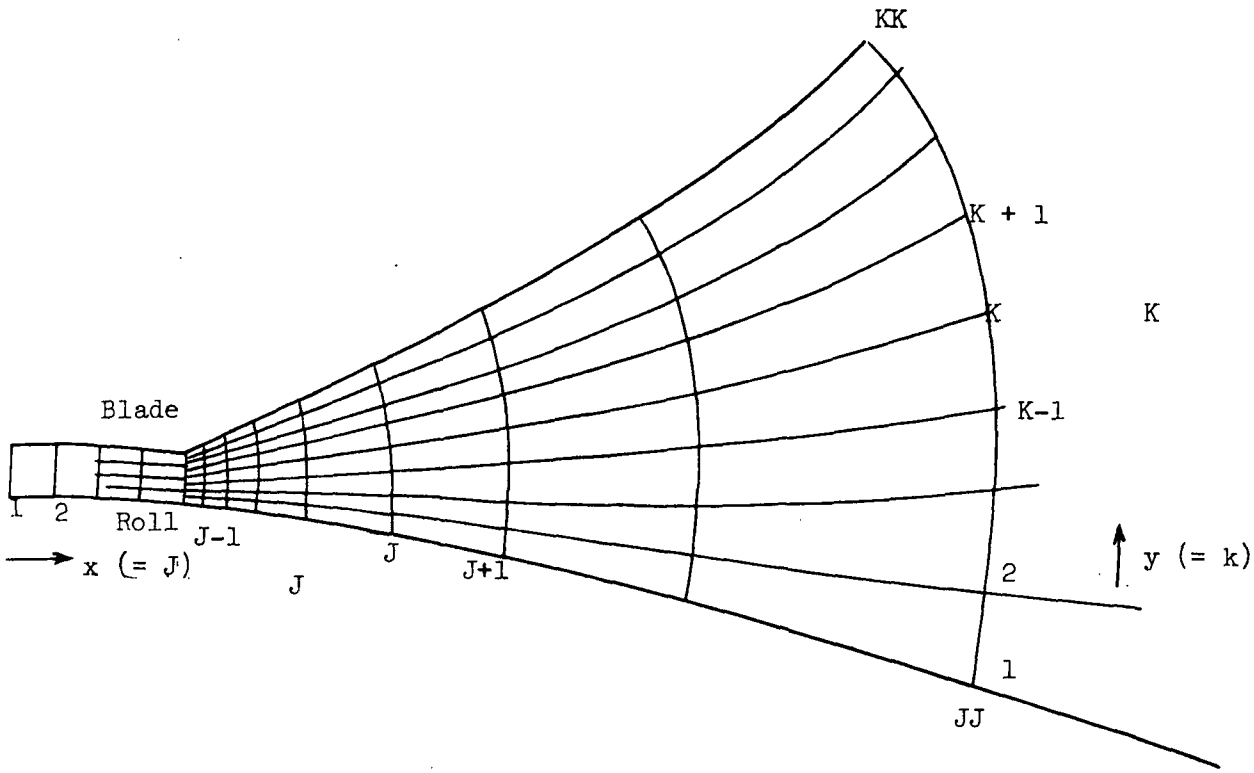

Figure 11. Orthogonal Coordinate Grid Imposed on Blade Nip

Since one is required to solve several highly nonlinear partial differential equations simultaneously, it is apparent that classical numerical techniques cannot be used. The various terms in the equations are separated into more important, or primary, terms and less important, or secondary, terms. By holding the secondary terms as constant functions of $\underline{x}$ and $\underline{y}$, the primary terms are solved to give complete profiles of $\underline{v}$ and τ_{11}. The secondary terms are then reevaluated and the process is repeated until a solution is obtained. A summary of the steps required is as follows:

(1) Lay out the coordinate system as indicated in Fig. 11 (mathematically, not graphically). Derive the metric components Δ and δ and their required derivatives.

(2) Estimate initial values for $\underline{u}(\underline{x},\underline{y})$, $\underline{v}(\underline{x},\underline{y})$, $\overline{\eta}(\underline{x},\underline{y})$, $\tau_{11}(\underline{x},\underline{y})$, and $\underline{q}$ (the net volumetric flow rate through the nip). This is done by assuming viscometric flow.

(3) The equations to be solved are (8), (9), (19), (20), (42), and (44), plus the equation for $\underline{q}$:

$$q = -\int_{1}^{KK} \delta v dy = \text{constant.} \qquad (\quad$$

The primary terms are $\partial\tau_{11}/\partial x$, $\partial\tau_{11}/\partial y$, $\partial^2 v/\partial x^2$, and $\partial^2 v/\partial y^2$. All other terms are evaluated using current variable values. The resulting two equations to be solved are:

$$\partial\tau_{11}/\partial y = f_1(x,y) \qquad (\quad$$

$$\partial\tau_{11}/\partial x + (\overline{\eta}\Delta/\delta^2)\ \partial^2 v/\partial y^2 - (\overline{\eta}/\Delta)\ \partial^2 v/\partial x^2 = f_2(x,y). \qquad (\quad$$

(4) It is possible to simplify the problem by replacing the term $\partial\tau_{11}/\partial x$ in Equation (49) by a variable which is a function of $\underline{x}$ only. This is done as follows. First, on each line $\underline{J}$ evaluate a new function:

$$f_3(x,y) = \int_{1}^{K} f_1(x,y)\ dy. \qquad (\quad$$

Derive an estimate of the new values of τ_{11} on line $\underline{J}$, $\tau_{11})_e$:

$$\tau_{11})_e = \overline{\tau_{11}} - \overline{f_3} + f_3(x,y) \qquad (\quad$$

in which $\overline{\tau_{11}}$ is the average current value of τ_{11} on line $\underline{J}$ and $\overline{f_3}$ is the average value of $\underline{f_3}$ on line $\underline{J}$. $\tau_{11})_e$ is composed of secondary terms only and is thus constant in this part of the calculations. Since Equation (48) must be satisfied, the true next values of τ_{11} must be $\tau_{11})_e$ plus some variable which is a function of $\underline{x}$ only, as follows:

$$\tau_{11})_n = \tau_{11})_e + g_1(x). \tag{52}$$

Equation (52) is substituted into Equation (49) to give:

$$(\bar{\eta}\Delta/\delta^2)\,\frac{\partial^2 v}{\partial y^2} - (\bar{\eta}/\Delta)\,\partial^2 v/\partial x^2 + g(x) = f_4\,(x,y) \tag{53}$$

in which $\underline{f_4}(\underline{x},\underline{y})$ is a new function composed of secondary terms only and $\underline{g}(\underline{x})$ is a function to be determined as part of the calculation. The relationship between $\underline{g}(\underline{x},\underline{y})$ and $\underline{g_1}(\underline{x},\underline{y})$ given by Equation (54) is used later to evaluate the new values of $\tau_{11}(\underline{x},\underline{y})$.

$$g\,(x,y) = \frac{d}{dx}\,g_1(x). \tag{54}$$

On each line $\underline{J}$ (that is, at each value of $\underline{x}$) Equation (53) is solved for $\underline{v}(\underline{x},\underline{y})$ and $\underline{g}(\underline{x})$ subject to the velocity boundary conditions and Equation (47). It can be shown that this is an exact solution and is not subject to trial and error methods.

The procedure is repeated on all lines $\underline{J}$ until acceptable constant functions for $\underline{v}(\underline{x},\underline{y})$ and $\underline{g}(\underline{x})$ are obtained. This is a trial and error procedure in the $\underline{x}$ direction but not in the $\underline{y}$ direction.

(5) New values of τ_{11} are determined as follows:

$$\tau_{11})_{new} = \tau_{11})_e + \int_1^J g(x)\,dx + \text{constant}. \tag{55}$$

The constant in Equation (55) is determined by fixing the proper boundary condition for τ_{11} at $\underline{x} = \underline{J} = 1$.

(6) The boundary condition for τ_{11} will in general not be satisfied at $\underline{x} = \underline{JJ}$, and this difference is used to estimate a new volumetric flow rate $\underline{q}$.

For viscometric flow this would be equivalent to adjusting the flow rate up or down to make the pressure equal to zero at the nip inlet and outlet.

(7) The velocity $\underline{v}(\underline{x},\underline{y})$ is adjusted on each line $\underline{J}$ to conform to the revised flow rate while retaining the shape of the velocity profile.

(8) The equation of continuity, Equation (17), is used to evaluate ne values of $\underline{u}(\underline{x},\underline{y})$.

(9) New estimates of all of the secondary terms are determined, and t calculations are returned to (3) for another trial.

ACKNOWLEDGMENTS

Dr. Richard Nelson made several useful suggestions in formulating the revised theory in proper tensor notation.

Thanks are due Mr. Marvin Filz, Mr. Robert Rae, and Mr. Keith Hardacker for their efforts in designing the new rheometer which is under construction.

FUTURE WORK

The two major aspects of the program to be followed in the next six months are experimental coating evaluation and the interpretation of experimental results. The most immediate concern is to continue the theoretical development as an aid in interpreting results. Success in this aspect of the program would permit one to use optimum experimental techniques in coating evaluation. Without a means of interpreting results one is forced into an endless investigation of coatings using different experimental parameters, without ever being sure how the results obtained in one experiment apply to another or to coater operation.

The results obtained to date using a wide angle blade (45°) were rather poor in quality and would not be acceptable in a detailed investigation of the effects of coating formulation. It will be determined in early experiments whether this is due to a faulty dial indicator. If so, additional work will be done with the 45° blades; if not, coating evaluation will be conducted with the previously used 10° blades.

The new rheometer is expected to be available in a minimum of two to three months. It will be evaluated for continued studies. It is expected that the new machine will have more flexibility in operational parameters and give higher quality results than the present instrument and, if so, it will be used in continued coating studies.

LITERATURE CITED

1. Ginn, R. F. and Leekley, R. M. A fundamental rheological study of the blade coating process. Project 3069, Progress Report One, The Institute of Paper Chemistry, July 27, 1973.

2. Research Proposal No. 2185, an extension of Project 3069, The Institute of Paper Chemistry, October 23, 1973.

3. Spiegel, M. R. Vector analysis and an introduction to tensor analysis. Schaum's Outline Series. New York, Schaum Publishing Co., 1969.

4. Flügge, W. Tensor analysis and continuum mechanics. New York, Springer-Verlag, 1972.

5. Aris, R. Vectors, tensors, and the basic equations of fluid mechanics. Englewood Cliffs, N.J., Prentice-Hall, Inc., 1962.

6. Ginn, R. F. In Physical chemistry of pigments in paper coatings. TAPPI Monograph, C. Garey, ed. To be published.

THE INSTITUTE OF PAPER CHEMISTRY

Robert F. Ginn
Research Fellow
Division of Natural
Materials & Systems

Gary A. Baum
Group Coordinator
Division of Natural
Materials & Systems